

A method of simultaneous measurement of specific heat and thermal conductivity of solids near phase transition*

M. P. SINHA AND AMITABHA PAL

Department of Physics, Indian Institute of Technology, Kharagpur-721302

(Received 4 December 1975)

A method of simultaneous measurement of specific heat and thermal conductivity of solids using discontinuous heating technique is described. The measurement of specific heat of ammonium chloride between the temperature interval 90-300°K has shown an agreement with Ruhmann *et al*'s data within one percent. A phase transition has been observed at the temperature $231 \pm 2^\circ\text{K}$ from the temperature variation of specific heat and thermal conductivity of $\text{MnSiF}_6 \cdot 6\text{H}_2\text{O}$.

1. INTRODUCTION

In all types of calorimetry, the accuracy is limited by the loss of heat from the calorimeter to the surroundings. In isothermal calorimetry, this limitation is overcome to some extent by correcting the error due to heat loss to certain degrees of approximation. In adiabatic calorimetry, the heat loss is minimised by surrounding the calorimeter with a shield, whose temperature is regulated so as to be nearly equal to that of the calorimeter. Dauphinee *et al* (1954), in their continuous heating type specific heat apparatus, fed the temperature difference between the calorimeter and the shield to the shield temperature regulating device so as to null this temperature difference. Stout *et al* (1954, 1960) designed a discontinuous heating type specific heat apparatus and followed a graphical method of correcting the radiation loss. The authors have followed both the radiation shield method and the radiation correction method in their discontinuous heating type calorimetric apparatus for the simultaneous measurement of specific heat and thermal conductivity of solids in the temperature range 90-300°K.

2. EXPERIMENTAL

A specially designed cylindrical silver calorimeter (figure 1(a), of external diameter 2.5 cm, wall thickness 0.025 cm and length 3.2 cm has been used for the purpose. The calorimeter is provided with a central well, of diameter 1 cm and length 3 cms which encloses a formerless heater-thermometer of resistance 36.872 Ω at 0°C made of 39 S.W.G. suprenamelled commercial copper wire, whose temperature resistance characteristic has proved to be reproducible within

*A part of the work was reported in the *First National Symposium on Cryogenics* at I.I.T., Kharagpur.

limits of error (Dauphinee *et al* 1954). A calibrated copper constantan thermocouple soldered with Woods metal with the outer surface of the calorimeter is used as primary standard against which the resistance thermometer is calibrated. The calorimeter is surrounded with a massive radiation shield, provided with a heater made of Karma wire, which in turn is placed inside a vacuum chamber (10^{-5} mm of Hg). Liquid nitrogen is used as the refrigerant.

Both the power input and the increase in temperature in the heater—thermometer are measured with the same circuit which basically consists of two potential lead resistors connected in series with a constant voltage source. One of these resistors is the copper thermometer-heater, whose resistance is measured by using an X—Y recorder (sensitivity 10 micro-volt/mm). The other resistor is for the measurement of current which is read in digital multimeter (sensitivity $1\mu\text{A}$). The temperature of radiation shield is regulated manually so as to be close to the equilibrium temperature in course of a single measurement.

3. METHOD OF MEASUREMENT

In an adiabatic determination of heat capacity, the distribution of heat supplied to a system comprising the sample and calorimeter, is expressed as

$$\Delta Q = mC_p\Delta T + C\Delta T \quad \dots (1)$$

where ΔQ is the total heat supplied, ΔT is the effective rise in temperature of system, m is the mass of the sample, C_p is the specific heat of the sample and C is the thermal capacity of the calorimeter.

For accurate determination of ΔT , the heat loss to the surroundings as well as the relaxation effect between the sample and its container are considered by taking into account the transfer of heat between the calorimeter and the sample through the conductance h_1 and that between the calorimeter and its surroundings through the conductance h_2 as indicated by the heat flow diagram (figure 1(b)). The corresponding equation of heat transfer is

$$-C \frac{dT_c}{dt} = h_1(T_c - T_s) + h_2(T_c - T_s) \quad \dots (2)$$

where T_c and T_s are the instantaneous temperatures of the calorimeter and the sample respectively and T_s is the temperature of the radiation shield in the rating period after a heat pulse is given to the calorimeter. Considering the case, in which the final temperature of the calorimeter is nearly equal to the temperature of the radiation shield and neglecting any loss, to the shield, which is very small under these circumstances (Parkinson *et al* 1954)

$$C(T_c - T_s) = mC_p(T_s - T) \quad \dots (3)$$

for all temperature ranges.

The equation of heat transfer then becomes

$$\frac{dT_c}{dt} + \beta(T_c - T_s) = 0 \quad \dots (4)$$

where

$$\beta^{-1} = \frac{CmC_p}{h_1(C + mC_p)} \quad (5)$$

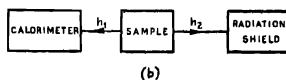
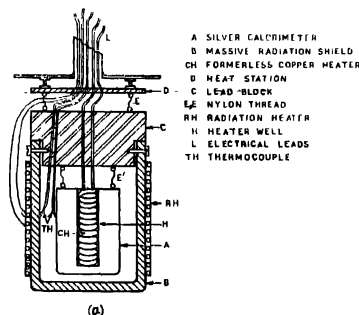


Fig. 1. (a) Schematic diagram of the calorimeter
(b) block diagram of heat flow

The solution of eq. (4) is

$$(T_c - T_s) = (T_c^m - T_s)e^{-\beta t} \quad \dots (6)$$

where T_c^m is the instantaneous temperature of the calorimeter just at the end of the heat pulse. The relaxation time constant β^{-1} in eq. (6) is the time taken by the system in attaining the equilibrium temperature and can be determined from the equation

$$\ln (T_c - T_s) = \ln (T_c^m - T_s) - \beta t. \quad (7)$$

Figures (2) and (3) are the typical plot of T_c vs t and $\ln (T_c - T_s)$ vs t respectively in the fore rating period and after rating period for a sample which has a phase transition point at $231 \pm 2^\circ\text{K}$. Figures indicate that the experimental curves follow the derived time temperature equation. The relaxation time β^{-1} for each heat pulse is determined from the slope β of the respective straight line

of figure (3) The final equilibrium temperature between the calorimeter and the sample is then recognised from figure (2), as the value of T_e at $t = \beta^{-1}$.

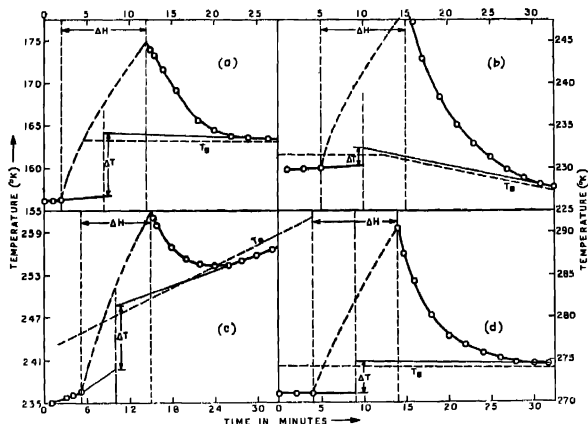


Figure 2. Time vs temperature plots (a, c, d) in different conditions of the shield temperature, and (b) at the transition point.

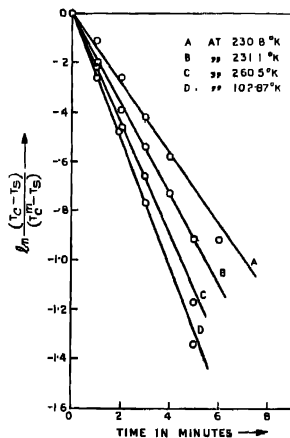


Fig. 3. $\ln \left(\frac{T_0 - T_e}{T_e^m - T_e} \right)$ vs time plot at different mean temperatures

Plots in figure 2 are the time variation of the calorimeter temperature T_c with different conditions of the shield temperature T_s . The figures show that after the relaxation period the calorimeter temperature T_c decreases or increases with time according as the shield temperature is lower or higher than the equilibrium temperature between the calorimeter and the sample. Figure 2(b) is the time temperature plot near the transition point, which shows that shield temperature starts falling though the constancy in the heat input to the shield is maintained. It appears that sample in the transition region becomes heat sink. Actual rise in temperature (ΔT) of the system comprising the sample and the calorimeter is therefore determined graphically by the same method as was followed by Stout and others (1960) and is then used in eq (1) to calculate the specific heat C_p of the sample.

Thermal conductance, h_1 between the calorimeter and the sample for a particular mean temperature is determined from the relation

$$h_1 = \frac{CmC_p}{C + mC_p} \beta \quad \dots (8)$$

which is then used to determine the thermal conductivity K of the sample from the expression

$$K = \frac{h_1}{2\pi l} \left(\frac{r_2}{r_2^2 - r_1^2} \right) \left[\frac{r_2^2 - r_1^2}{2} - r_2^2 \ln \frac{r_2}{r_1} \right] \quad \dots (9)$$

found from the unsteady state cylindrical heat flow equation (Bech *et al.*, 1974). Where r_1 , r_2 and l are respectively internal diameter, the external diameter and the length of the cylindrical sample chamber.

4. STANDARDISATION OF THE APPARATUS

Standardisation of the apparatus was done by measuring the specific heat of analar quality polycrystalline ammonium chloride in the temperature range 90-300°K. The variation of C_p with temperature through the transition is shown in figure 4 in which the \circ represent the present data and \otimes are plotted from the Simon, Von Simpson and Ruheman's data (1927) for comparison. It may be noted that the present specific heat data shown in figure 4 coincide with the earlier data within one percent which in the present case is the experimental uncertainty. The transition temperature $T_c = 242.4^\circ\text{K}$ not only agrees with the earlier observation but also the shape of the specific heat curve at the transition region is obtained.

5. MEASUREMENT OF C_p AND K OF $\text{MnSiF}_6 \cdot 6\text{H}_2\text{O}$

The temperature dependence of heat capacity and thermal conductivity of $\text{MnSiF}_6 \cdot 6\text{H}_2\text{O}$ in the temperature interval 90-300°K are shown in figure (5a and 5b). The single crystals of $\text{MnSiF}_6 \cdot 6\text{H}_2\text{O}$ were prepared by dissolving MnCO_3 ,

freshly prepared silica gel in dilute HF and slowly evaporating the solution in a vacuum desiccator. We have measured the heat capacity of the sample because the optical data of Tsukawa & Courture (1955) have suggested that the single crystals of $\text{MnSiF}_6 \cdot 6\text{H}_2\text{O}$ undergo the structural transition below about 225°K .

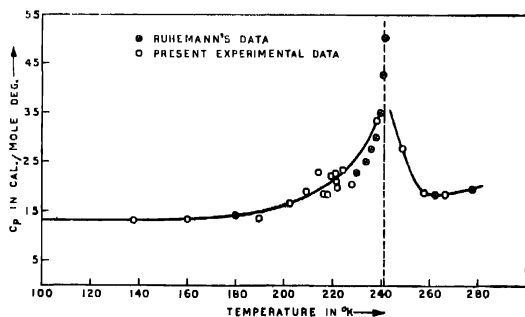


Fig. 4. Thermal variation of molar specific heat of NH_4Cl at low temperatures, O represents present data, \otimes represents Simon, Simson and Ruheman's data.

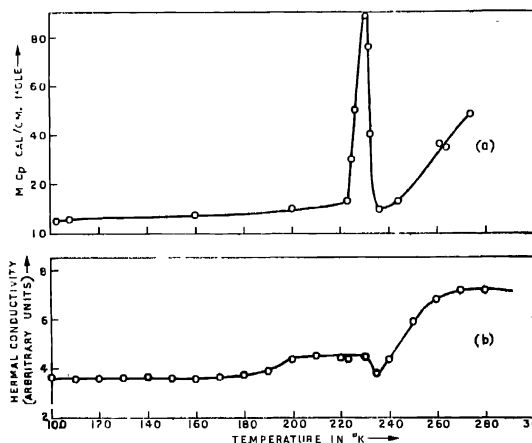


Fig. 5. Thermal variation of (a) molar specific heat and (b) thermal conductivity at low temperatures.

The curve 5a shows that an anomaly in the specific heat is present in the temperature region $223\text{--}268^\circ\text{K}$. The specific heat maximum occurs at $231 \pm 2^\circ\text{K}$. The reversible nature of the transition is ascertained by measuring the specific heat after the sample is taken through the thermal cycling several times.

The temperature dependence of thermal conductivity of $\text{MnSiF}_6 \cdot 6\text{H}_2\text{O}$ is shown in figure (5b). It is evident from figure (5b) that at the transition point $T(c) = 231 \pm 2^\circ\text{K}$ there is a dip in the curve and the thermal conductivity abruptly decreases which is qualitatively in agreement with the variation of thermal conductivity of CoO and NiO at the transition points measured by Lewis & Saunders (1973).

6. CONCLUSION

The present experiment measures simultaneously the specific heat and the thermal conductivity of solids at the phase transition points. Both in case of NH_4Cl and $\text{MnSiF}_6 \cdot 6\text{H}_2\text{O}$ the absolute value of the specific heat and the thermal variation of the specific heat has an error of about one percent. The temperature variation of the thermal conductivity for the unsteady state heat conduction has been obtained within an accuracy of one percent. It is inherent in the method of measurement that the absolute value of thermal conductivity at room temperature has an accuracy about five percent.

ACKNOWLEDGMENTS

It is a real pleasure to acknowledge our gratitude to Professor S. K. Dutta Roy for introducing us to this problem and for his constant encouraging guidance.

REFERENCES

- Bech J. V. & Arai, S. A. 1974 *Jour. of Heat Transfer*, **96**, 59.
 Cole, A. G. Hitchens J. D. Robie R. A. & Stout J. W. 1960 *J. Am. Chem. Soc.* **82**, 4807.
 Dauphinee, T. M., MacDonald D. K. C. & Thomas II 1954 *Proc. Roy. Soc. A* **221**, 267.
 Parkinson D. H. & Quarrington J. E. 1954 *Proc. Phys. Soc. (London)* **A 67**, 569.
 Stout, J. W. 1954 *Rev. Sci. Instr.* **25**, 920.
 Simon F., Simon, O. V. & Ruhemann M. 1927 *Z. Physik Chem.*, **129**, 339.
 Tsujikawa J. & Courture L. 1955 *J. de Phys. Rad.* **16**, 430 (Quoted by Ohtsubo, A. 1965 *J. Phys. Soc. Japan*, **20** No. 1, 82).
 Lewis F. B. & Saunders N. H. 1973 *J. Phys. C*, **6**, 2525.